The influence of time varying magnetic fields on the determinations of Newton's constant at the Bureau International des Poids et Mesures

Speake, Clive C; Bryant, John L; Davis, Richard S; Quinn, Terry J

DOI:
10.1088/1681-7575/acb69a

Document Version
Publisher's PDF, also known as Version of record

Citation for published version (Harvard):
Speake, CC, Bryant, JL, Davis, RS & Quinn, TJ 2023, 'The influence of time varying magnetic fields on the determinations of Newton's constant at the Bureau International des Poids et Mesures', *Metrologia*, vol. 60, no. 2, 024001. https://doi.org/10.1088/1681-7575/acb69a

The influence of time varying magnetic fields on the determinations of Newton's constant at the Bureau International des Poids et Mesures

OPEN ACCESS
IOP Publishing | Bureau International des Poids et Mesures Metrologia
Metrologia **60** (2023) 024001 (11pp) https://doi.org/10.1088/1681-7575/acb69a

The influence of time varying magnetic fields on the determinations of Newton's constant at the Bureau International des Poids et Mesures

Clive C Speake[1,*], **John L Bryant**[1], **Richard S Davis**[2] and **Terry J Quinn**[2]

[1] School of Physics and Astronomy, University of Birmingham, Edgbaston, Birmingham B15 2TT, United Kingdom
[2] Bureau International des Poids et Mesures (BIPM), Pavillon de Breteuil, F-92312 Sèvres CEDEX, France

E-mail: c.c.speake@bham.ac.uk

Received 15 September 2022, revised 24 January 2023
Accepted for publication 27 January 2023
Published 16 February 2023

Abstract

The values of Newton's constant of gravitation, G, reported by determinations at the International Bureau of Weights and Measures (BIPM) in Quinn *et al* (2001 *Phys. Rev. Lett.* **87** 111101/1–111101/4) and in Quinn *et al* (2013 *Phil. Trans. R. Soc. A* **372** 2–28) are some 200 parts per million (ppm) larger than the value of 6.67430×10^{-11} m^3 kg^{-1} s^{-2} which was recommended by CODATA in Tiesinga *et al* (2018 *J. Phys. Chem. Ref. Data* **50** 033105). The CODATA value has an assigned uncertainty of 22 ppm and the reported uncertainties in the BIPM values were 41 ppm and 25 ppm, respectively. The discrepancy therefore amounts to about seven times the combined uncertainty of the latest BIPM and CODATA values. We examine experimentally the hypothesis that the difference is due to a bias produced by stray alternating (AC) magnetic fields in the vicinity of the experiment. Whilst the BIPM torsion balance was located at the University of Birmingham a coil, having a similar scale to the balance, was used to generate AC magnetic fields of magnitude approximately 1 μT which in turn produced torques of magnitude approximately 0.2 % of the gravity torque. The magnitudes of these torques were compared with simple analytical models and finite element analyses. Measurements in the laboratory in Birmingham and, more recently, at BIPM give a very conservative upper limit on the rms magnitude of ambient AC magnetic fields of 100 nT. As the torque was demonstrated to vary with the square of the ambient field, these observations and our analyses suggest an upper limit to the possible bias in the BIPM determinations of the order of 20 ppm. It is therefore unlikely that torques due to ambient magnetic fields could have significantly biased values of G determined at BIPM.

* Author to whom any correspondence should be addressed.

Keywords: forces due to eddy current forces, Newton's constant of gravitation, BIPM determination of G

(Some figures may appear in colour only in the online journal)

1. Introduction

It is well known that recent independent determinations of Newton's constant of gravitation, G, have reported values that have differences that are significantly larger than their stated uncertainties. This situation is reviewed in the following [4–7]. The values resulting from the work performed at the International Bureau of Weights and Measures (BIPM) [1, 8] are some 200 parts per million (ppm) larger than the CODATA's current recommended value but were reported with uncertainties of 41 and 25 ppm respectively. However the result of 2013 was consistent with the earlier value and was derived from a similar but significantly improved apparatus [2]. In addition, each of these determinations was derived from a combination of two methods of measurement taken with the same torsion-strip balance: one employing an electrostatic feedback and the other using the free-deflection of the balance.

It is important to highlight a number of features of the design of the experiment for the purposes of this article. A plan view of the basic geometry of the source and test masses used in both the BIPM determinations is shown in figure 1. Both test and source masses were manufactured from copper-tellurium alloy, having magnetic susceptibility and electrical conductivity similar to those of pure copper and had mass values which were approximately 1.2 and 11.2 kg respectively. The heights and diameters of the masses were approximately equal and approximately 55 and 118 mm, respectively. The test masses were suspended from the balance (not shown in the figure). The low magnetic susceptibility of the masses eliminates spurious torques due to static magnetic fields and gradients. The value of G was derived from the difference between the maximum positive and maximum negative torques exerted on the torsion balance with the source masses at $\pm\theta_m$ as indicated in figure 1. The radial distances of the test and source masses from the axis of rotation of the torsion balance were 120 mm and 213 mm respectively. The separation between the centres of the source and test masses at the extrema of the torque is approximately 107 mm corresponding to a rotation of the source masses about the axis of rotation of $\theta_m \approx 19°$ and an angle $\theta_s \approx 41°$ between the mass centres as indicated in figure 1. The torsion balance and the suspended test masses were located in a vacuum chamber constructed from aluminium alloy and the source masses were located on a carousel exterior to the vacuum chamber which was also constructed from aluminium alloy. During both of the BIPM determinations the complete experiment was mounted on the working surface of a coordinate measuring machine (CMM). The CMM in the second measurement was of similar design to the first but of higher specification.

The test mass values are considerably larger than those used in other determinations that use torsion balances resulting in a significantly larger gravitational torque, of about 3×10^{-8} N m peak-peak[3]. This advantage follows from the properties of a torsion strip (see [2] and references therein). The wall of the vacuum chamber has a thickness of about 4 mm over the vertical extent of the source masses to enable the source and test masses to be in close proximity and to achieve as large a gravitational torque signal as practical. The chamber thickness elsewhere is about 22 mm (see section 2 below). Due to the proximity of the source and test masses it was not feasible to install a ferromagnetic shield around the test mass assembly, as is usually desirable. The late Bryan Kibble pointed out [9] that, in the absence of such shielding, it was possible that ambient alternating magnetic fields due to local instruments and local mains wiring, for example, could create eddy current flows in the masses that in turn could give rise to spurious magnetic torques. It seemed likely that such torques would be attractive and would bias the deduced value of G in the direction that could account for the current apparent conflict. The aim of the work reported here is to establish the plausible magnitude of such a potential bias in the BIPM determinations of G.

2. The BIPM torsion balance at the University of Birmingham with a local source of alternating magnetic field

In 2015, the BIPM torsion balance was installed at the University of Birmingham in a dedicated basement laboratory on a slate slab (see figure 2) and housed in a temperature controlled polystyrene enclosure ($\pm$0.01 K) with a nominal control temperature of 23 C. A rectangular coil was constructed with the normal to its plane in the horizontal direction and fitted so that it straddled the working torsion balance as indicated in figure 1. The coil of 9 turns was wound on a plastic former that had a width of 0.674 m, a height of 1.17 m and the plane containing the centres of the masses was 0.48 m above the bottom horizontal part of the coil. In the absence of nearby conductors the coil produced at its centre an rms magnetic field of 0.86 μT for an amplitude of current of 1 A. With the coil in place on the apparatus, an AC gaussmeter was mounted on top of the vacuum can and measured a rms field of 1 μT for an amplitude of current in the coil of 0.11 A at a frequency of 60 Hz. A view of the experiment after removal of the vacuum chamber in shown in figure 3.

Measurements of the ambient fields were made with the gaussmeter which had a fluxgate probe and which recorded rms fields over a bandwidth from 15 Hz to 10 kHz with a resolution of 2 nT. In trying to characterise the ambient alternating

[3] We describe the magnitude of oscillating quantities later as peak values. That is simply half their peak-peak value.

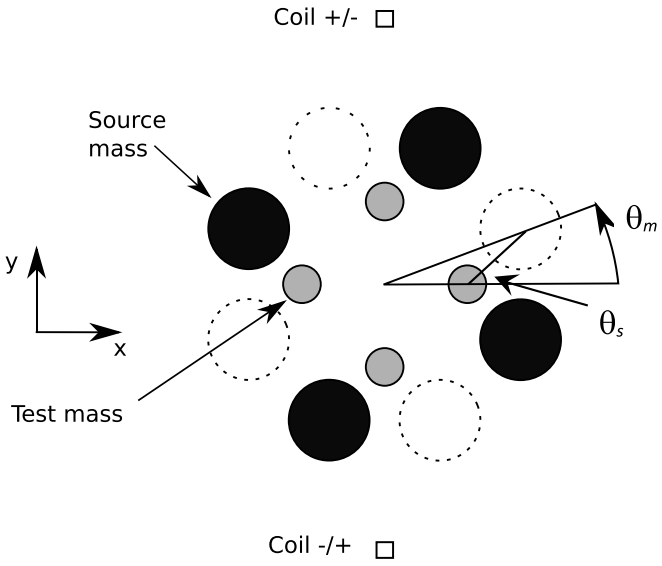

Figure 1. A plan view of the geometry of the test and source masses used in the BIPM determinations of Newton's constant. Torques were observed with the source masses rotated on a carousel between positions where they produce maxima/minima corresponding to approximately $\theta_m \approx \pm 19^\circ$ (positions indicated as black-filled or dotted outlines). The test masses are grey-filled and are attached to a torsion strip balance inside a vacuum chamber which is not shown and the drawing is to scale. The cross section through the vertical windings of the rectangular coil, added to the BIPM apparatus for the purposes of this study, are also indicated.

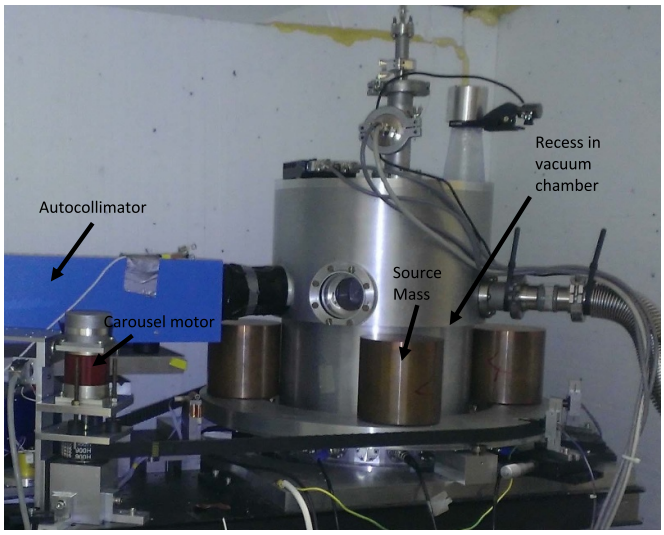

Figure 2. View of the BIPM torsion balance whilst it was set up at University of Birmingham. The source masses and the recesses in the vacuum chamber can be clearly seen.

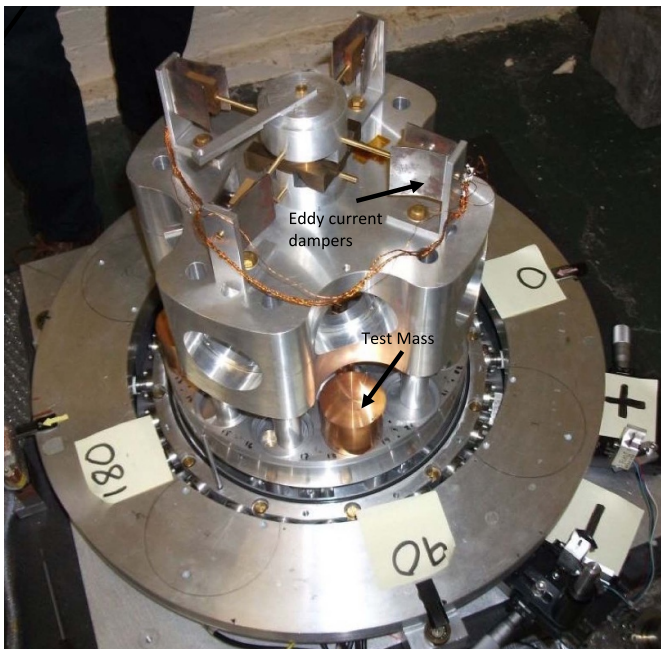

Figure 3. The torsion balance assembly with test masses after having removed the lid of the vacuum chamber. The 'cross' assembly supports the torsion strip and is an eddy current damper.

magnetic fields it was useful to think of them as arising from two types of source. One class of source comprised compact and nearby electronic components that produce inhomogeneous fields at the torsion balance. The second class are large scale sources, such as power lines running in the walls of the laboratory, whose fields are more homogeneous. We surveyed the magnetic environment of the experiment before and after dismantling the experiment to ship it to the National Institute of Standards and Technology (NIST) in the USA in March 2016. We concluded that the field due to compact local sources was about 10 nT, which came from the power supplies located on a rack located about 2 m away from the centre of the vacuum can, and a roughly equal amount came from a background that was approximately spatially constant in the vicinity of the experiment. The field rose to about 150 nT at the rack containing all the electronics required to run the experiment. The angular position of the torsion balance was recorded with the Elcomat autocollimator that was used in the determination reported in [2]. No significant alternating magnetic fields were found associated with the auto-collimator. A turbo pump was located at a distance of 2 m from the apparatus. This created an AC magnetic field of a maximum of 130 nT as the turbo pump spun down after switch off but, whilst running at full speed (1 kHz), the magnetic field at the pump was measured to be 70 nT. The quiescent field in the stepper motor drive for the carousel was not significant.

In the next two sections we will describe analytical methods for estimating the torque due to AC magnetic fields. We will compare these predictions and results from finite element analyses (FEA using ANSYS Maxwell) to experimental measurements in section 5 below.

3. The torques acting on the torsion balance due to an oscillating magnetic field

3.1. Analytical model

The starting point for the analysis [10] is to consider the interaction energy, W_{st}, between two pure magnetic dipoles, $\vec{p}_{s,t}$

where the subscripts indicate the source or test mass in an obvious way, and where,

$$W_{st} = \frac{\mu_0}{4\pi r_{st}^3}\left(\vec{p}_s \cdot \vec{p}_t - 3\left(\hat{n}_{st} \cdot \vec{p}_s\right)\left(\hat{n}_{st} \cdot \vec{p}_t\right)\right), \tag{1}$$

with $\vec{r}_{st} = \vec{r}_t - \vec{r}_s$, $r_{st} = |\vec{r}_{st}|$ and $\hat{n}_{st} = \vec{r}_{st}/r_{st}$.

We will assume that the dipole moments of the source and test masses are induced by the external oscillating fields, $\vec{B}_{s,t}$, at their respective locations. We can then use the analysis given by Smythe [11] to calculate their dipole moments. This analysis assumes that the electric and magnetic fields are 'instantly propagated' in the words of Smythe, which is equivalent to the wavelength of electromagnetic radiation at the frequency of interest being much larger than the dimensions of the region of interest. In our study an upper frequency limit of 400 Hz is adequate and we can therefore clearly ignore propagation effects. Assuming that the masses are spherical with radii $a_{s,t}$, of relative permeability μ_r, electrical conductivity σ, their magnetic moments can be written form as:

$$\vec{p}_{s,t} = |d_{s,t}|\vec{B}_{s,t}\cos\left(\omega t + \beta_{s,t}\right), \tag{2}$$

where $\vec{B}_{s,t}$ are the peak amplitudes of field and the $|d_{s,t}|$ are the moduli of complex quantities,

$$d_{s,t} = \frac{1}{2}\frac{4\pi}{\mu_0}\frac{\left(2\mu_r+1\right)v_{s,t} - \left[\left(1+v_{s,t}^2\right)+2\mu_r\right]\tanh\left(v_{s,t}\right)}{\left(\mu_r-1\right)v_{s,t} + \left[\left(1+v_{s,t}^2\right)-\mu_r\right]\tanh\left(v_{s,t}\right)}a_{s,t}^3. \tag{3}$$

The phase of the dipole moment relative to the polarising field, $\beta_{s,t}$, can be calculated in the usual way in terms of the real and imaginary components of $d_{s,t}$. The parameter $v_{s,t}$ is defined as:

$$v_{s,t} = \frac{(1+j)}{\delta}a_{s,t}, \tag{4}$$

where $j = \sqrt{-1}$ and the skin-depth is defined in the usual way as:

$$\delta = \left(\frac{2}{\omega\sigma\mu_0\mu_r}\right)^{1/2}. \tag{5}$$

The interaction energy from equation 1 can then be written in terms of unit vectors of the magnetic fields:

$$W_{st} = \frac{\gamma}{r_{st}^3}\left(\hat{B}_s \cdot \hat{B}_t - 3\left(\hat{n}_{st} \cdot \hat{B}_s\right)\left(\hat{n}_{st} \cdot \hat{B}_t\right)\right), \tag{6}$$

where γ is a function of the frequency of the magnetic field and the magnetic permeability, electrical conductivity and the radii of the masses. We define $\hat{B}_{s,t} = \vec{B}_{s,t}/|\vec{B}_{s,t}|$. In the case where B_s and B_t are in phase, we can take the time-averaged component of equation (6) and find,

$$\gamma = \frac{1}{2}\cdot\frac{2\pi}{\mu_0}|d_s||d_t|B_sB_t\cos\left(\beta_s - \beta_t\right). \tag{7}$$

This can be conveniently written for the more general case where the two magnetic fields have different phases as:

$$\gamma = \frac{1}{2}\cdot\frac{2\pi}{\mu_0}\mathrm{Re}\left\{d_tB_t \cdot \mathrm{conj}\left(d_sB_s\right)\right\}. \tag{8}$$

3.2. The forces acting between a source and test mass in a uniform field

We will initially consider a simple situation where a single test mass rotates around a single source mass in a uniform magnetic field, $\vec{B}_0$, so we now have $\vec{B}_s = \vec{B}_t = \vec{B}_0$ in the equations in section 3.1. In the case of only one pair of masses we can locate the source mass at the origin of the coordinate system. We can use the results of section 3.1 to find the forces acting on the test mass. Equation (6) becomes:

$$W_{ts} = \frac{\gamma}{r_{ts}^3}\left(1 - 3\cos^2\left(\theta - \phi\right)\right), \tag{9}$$

where θ is the rotation angle of the test mass and is defined as the direction of vector $\vec{r}_{ts}$ relative to the x axis and ϕ defines the direction of the magnetic field relative the x axis. We can find the forces acting in the $\vec{r}_{ts}$ direction and in the $\hat{\theta}$ direction by finding the derivatives of W_{ts} in the usual way.

A nominal value of conductivity of masses was taken to be 5.8×10^7 S m^{-1}. The uniform field was in the y direction and was oscillating at a frequency of 60 Hz with a peak amplitude of approximately 1.25 μT. Figures 4(a) and (b) are plots with $r_{ts} = 200$ mm of the x and y components of the forces calculated by both FEA and the analytical method outlined in section 3.1 above. Figures 5(a) and (b) show similar plots but for $r_{ts} = 100$ mm. We observe that the agreement between the results of the two methods for the larger radial distance (figures 4(a) and (b)) is quite good (although the FEA signal is more noisy). It is interesting to note that the forces can be attractive or repulsive. The dipoles can be considered to be parallel to each other and the field at any given time. This ignores any difference in sign between the direction of the fields due the phase angles of the dipole moments of the source and test masses with respect to the driving field (that are explicitly included in equation (7)). In figure 4(a), when the test mass starts at $\theta = 0$ (on the x axis) the x component of the force is positive, or repulsive. Clearly this is because we have adjacent 'like poles' leading to a repulsion in the x direction. As the test mass moves to 90° we have adjacent 'unlike poles' resulting in an attractive force (in the -y direction).

It is interesting to note that the agreement between the analytical theory and FEA (which models cylindrical masses) plots is better for the larger separation. Further investigation shows that the agreement increases as the spacing relative to the size of the source masses increases. The force

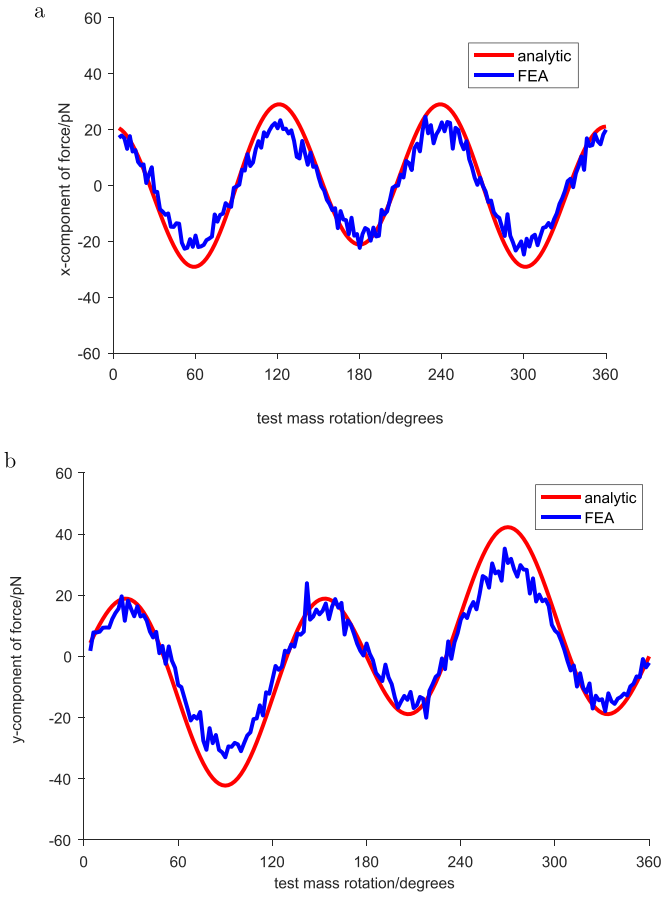

Figure 4. (a) and (b) Plots of the forces (x-component in 4a and the y component 4b) acting on the test mass as a function of its angular position with relative to the x axis. At an angle 90° the line joining the masses is parallel to the polarising magnetic field. The magnetic field has amplitude of 1.25 μT and frequency of 60 Hz. The distance between mass centres is 200 mm.

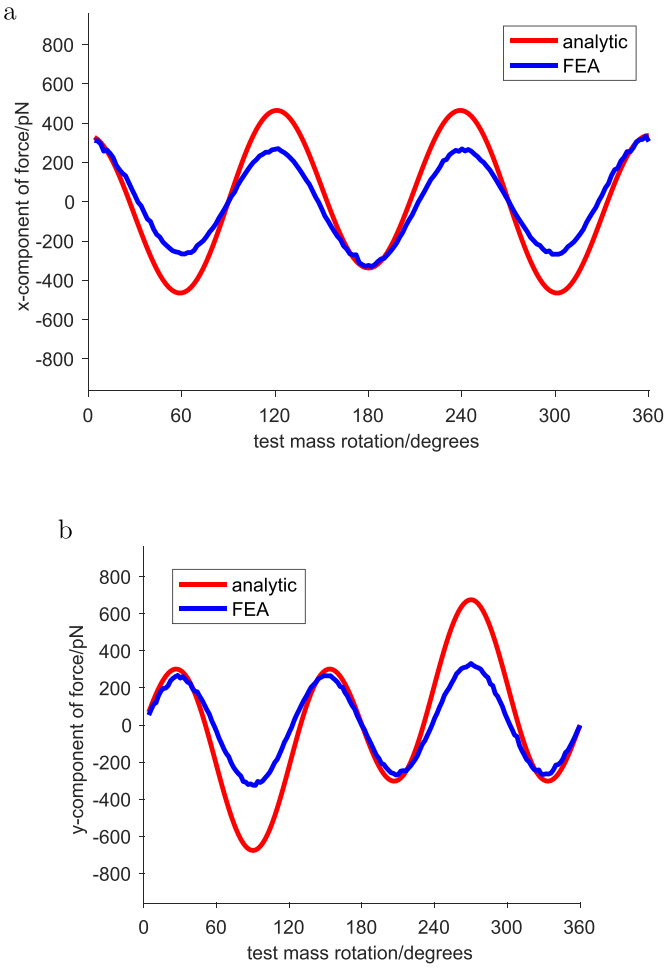

Figure 5. (a) and (b) Plots of the forces (x-component in 5a and the y component 5b) acting on the test mass as a function of its angular position relative to the x axis. At an angle 90° the line joining the masses is parallel to the polarising magnetic field. The magnetic field has amplitude of 1.25 μT and frequency of 60 Hz. The distance between mass centres is 100 mm.

varies as $1/r_{st}^4$ for larger separations and $1/r_{st}^3$ and for the opposite limit. In any case, for the purposes of this paper, we are only interested in predicting the magnitudes of the forces at the actual separation where the gravitational signal was measured (107 mm) where the model described here is adequate. We will adopt the equation of the energy given in equation (1) and we also note that the difference between the two models is insignificant ($\lesssim$10%) in the context of this paper. The peak-peak force is approximately 400 pN for mass separations of 100 mm which together with the radial distance of the test masses from the rotation axis of the torsion balance would be expected to give torques of order 0.4 nN m for all four masses (recall that the gravitational torque is approximately 30 nN m). This immediately suggests that electromagnetic torques could be of the order of 0.5 % for magnetic fields of 1.25 μT.

3.3. Calculation of the torque

We can proceed to estimate the torque due to the field of the coil on the complete balance using the dipole–dipole model. We use equation (9) to calculate the total interaction energy, Ω, of each test mass with every source mass using the direction and magnitude of the magnetic field at the locations of the masses. We use a coordinate system centred on the rotation axis of the torsion balance with:

$$\Omega = \sum_{i,j=1..4} W_{ij}(\theta_t), \tag{10}$$

where θ_t is the rotation angle of the torsion balance.

For a single mass pair the torque can be calculated by finding the derivative of the energy in 9,

$$\Gamma = -\frac{\partial W_{ts}}{\partial \theta}, \tag{11}$$

or

$$\Gamma = \frac{\gamma}{r_{st}^3}\sin 2(\phi - \theta). \tag{12}$$

The torque only depends on the difference between the angle of the position vector of the source mass relative to the

test mass and is periodic with twice this angle. In the case where we have four-fold symmetry, as is the case in the BIPM experimental configuration, the torques on the balance due to the four mass pairs will cancel for any value of θ_s. This is also true independently of the angle of the field relative to the orientation of the torsion balance, provided that the field is uniform over the balance.

In the experiment the field is not perfectly uniform and we expect the torque to be dominated by the interaction between the source and test masses closest to current carrying wires of the coil where the field is largest. These are the test and source masses at the top and bottom of figure 1. It is the repulsive dipole component force in the x direction that will be responsible for the torque which opposes the gravitational attraction between the masses.

In order to proceed to evaluate equation (10) we need to find the forces between the masses in the presence of the vacuum chamber.

4. Penetration of an AC magnetic field into the vacuum chamber

As described in section 2 the test masses are located in an aluminium alloy vacuum chamber. In order to calculate the torques acting between the source and test masses due to alternating magnetic fields we have to calculate the effect of the vacuum chamber due to its conductivity. A standard result [12] that, at first, appears to be useful for calculating the magnitude of the attenuation of the fields at the interior of the vacuum chamber is that the amplitude of an oscillating magnetic field, $B(t)$, measured at a depth t inside a metal decays exponentially according to:

$$B(t) = B(t_0)e^{-(t-t_0)/\delta}, \tag{13}$$

where $B(t_0)$ is the field measured at an arbitrary position within the medium and δ is the skin depth as defined in equation (5) where, for aluminium alloy we take μ_r to be unity. This standard solution ignores the effects of any boundaries on the amplitude of the magnetic field and only applies to the attenuation of the magnetic field *within* a slab of metal. Equation (13) fails to predict, even qualitatively, the frequency dependence of the torques that were measured, as described in section 5 below. At a basic level the skin-depth argument does not satisfactorily account for the increase in the magnitude of the field external to the chamber which must occur in the limit of the skin depth becoming small compared with the chamber wall.

A more complete calculation is required that takes account of the fact that the vacuum chamber is a cavity. A geometry that lends itself to this analysis is that of a hollow sphere. We can repeat the calculation described in Smythe [11] for a solid conducting sphere immersed in a uniform oscillating magnetic field but now include the effect of an internal spherical cavity. The boundary value problem can be solved in a straightforward way using the more general form for the vector potential within the shell which is given by Smythe [11]. In the case

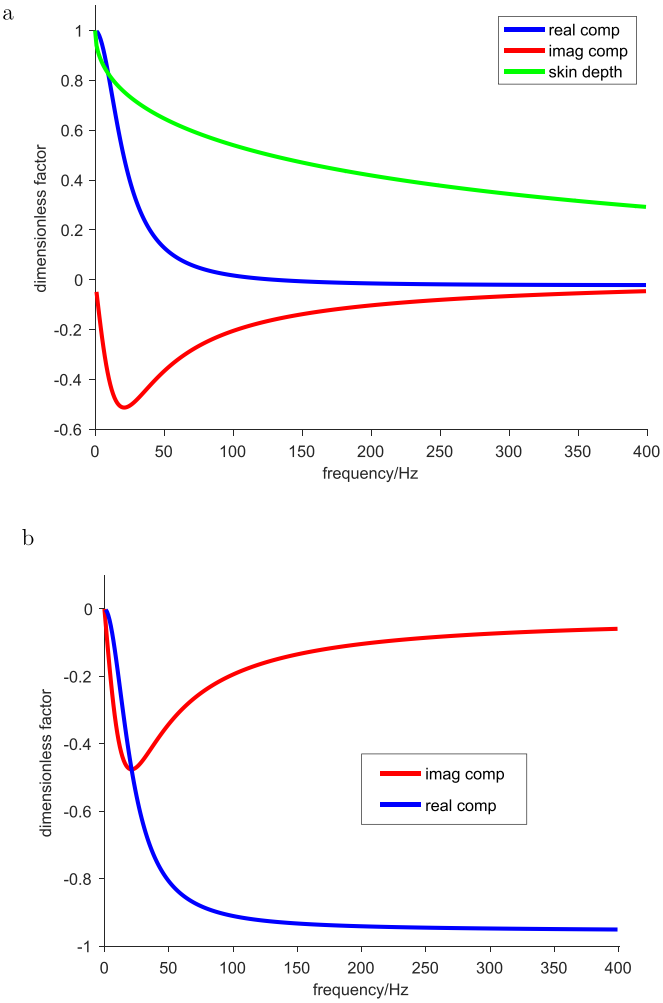

Figure 6. (a) Plots of the real and imaginary parts of the attenuation coefficient $A(\omega)$ given in equation (14). Also plotted is the attenuation predicted by the skin-depth argument (equation (13)) as discussed in the text. In figures 6(a) and (b) we assume that the conductivity is 1×10^7 S m^{-1}, the outer radius is 178 mm and the thickness is 4 mm. (b) Plots of the real and imaginary parts of the constant that determines the effective dipole moment of the vacuum chamber, $D(\omega)$, given in equations (15) and (16).

of a uniform external field, the field within the cavity is also uniform and is attenuated by a complex, dimensionless and frequency dependent factor,

$$\vec{B}_{int} = A(\omega)\vec{B}_0. \tag{14}$$

The form of $A(\omega)$ is unwieldy and we plot its real and imaginary parts in figure 6(a) together with the form of the attenuation factor for the skin depth given in equation (13). In figures 6(a) and (b) (discussed in the next paragraph), we assume the following values for the characteristics of the shell: the conductivity is 1×10^7 S m^{-1}, the outer radius is 178 mm and the thickness is 4 mm. The dimensions are the average radius of the vacuum chamber and the measured thickness of the thinnest section of its wall.

Now consider the external solution: the shell will generate a dipole moment (in a similar way to the masses as described in section 3) with an associated magnetic field. In this case we can express the final external field as the sum of the initial field and the radial (r) and polar (θ) components of the fields that are generated by the AC dipole moment of the shell. The final external field can then be written in terms of another frequency dependent constant, $D(\omega)$, with:

$$B_{ext\theta} = -B_0\left(1 - \frac{D(\omega)}{2r^3}\right)\sin\theta, \tag{15}$$

and

$$B_{extr} = B_0\left(1 + \frac{D(\omega)}{r^3}\right)\cos\theta, \tag{16}$$

where the factor $D(\omega)$ includes the effect of the cavity. The variation with polar angle θ of the magnitudes for the polar and radial components of the field of the shell is that expected from a simple dipole. Figure 6(b) plots the real and imaginary components of $D(\omega)/r^3$ where r is taken, for the purposes of the plot, to be the external radius of the shell.

We can define the dipole moment of the spherical shell using a parameter d_v that is analogous to d_{st} equation (3) where,

$$d_v = \frac{1}{2}\frac{4\pi}{\mu_0}D(\omega). \tag{17}$$

Given the result from Jackson [13] we can calculate the magnetic field at the position of the source mass due to the spherical shell,

$$\vec{B}_s(\vec{r}) = \frac{\mu_0}{4\pi r_s^3}\left(3\hat{n}_s(\hat{n}_s\cdot\vec{p_v}) - \vec{p_v}\right), \tag{18}$$

where $\vec{r}_s$ is the position of the source mass with respect to the centre of the vacuum chamber, $\hat{n}_s$ is the unit vector from the centre of the vacuum can to the source mass and $\vec{p}_v = d_v\vec{B}_0$. We then assume that this field is attenuated by the factor given in equation (14). We note however that this assumes that the field due to the source masses is uniform which clearly is not the case, so we cannot expect this model to accurately describe the geometry. We also assume that the centre of the hypothetical spherical shell is in the plane of the masses and on the torsion balance axis of rotation.

5. Comparison of observations and predictions

5.1. Analysis of torque vs current

Figure 7 shows the measured change in torque due to the applied AC magnetic field at 60 Hz versus the nominal peak coil drive current. The change in torque is calculated directly from the differences in the angular deflections recorded by the autocollimater and normalised by the nominal deflection due to gravity with no magnetic field applied. This is shown as a percentage in the plot together with 1 standard deviation limits that are magnified by a factor of 10. The sequence of torque values as a function of current, $\Gamma(i)$, can be represented as:

$$\Gamma(i) = \Gamma_G + kB_0^2 + kB_c^2, \tag{19}$$

where Γ_G is the torque due to gravity, B_0 is a background ambient field, B_c is the field due to the coil carrying current i and k is a constant. The ambient field would be expected to be at 50 Hz (UK mains frequency) and so it can be assumed that the torque due to this source is not coherent with that produced by the coil. We can fit the data to the following expression, which is valid for our case where the terms proportional to k are small,

$$R = \frac{\Gamma(i) - \Gamma(i=0)}{\Gamma(i=0)} = c_1 + c_2 i^2. \tag{20}$$

The parameter c_1 would be expected to remain zero if the background fields were constant over the period of about 2 weeks when the data were taken. The parameter $\Gamma(i=0)$ was taken as the first data point, which corresponded to zero current. Six data points were taken in total, with two at zero current. The uncertainty on each datum was calculated in the usual way. A plot of R, expressed in per-cent, versus current is shown in figure 7. The least squares analysis gives $c_1 = (0.9 \pm 1.3)\times 10^{-3}$ and $c_2 = -17.95 \pm 0.24$ (1 standard deviation).

These results clearly demonstrate that the torque scales with the square of the current in the coil, and therefore the square of the ambient alternating magnetic field, as expected from the analysis is section 3.1. The finite value of c_1 could correspond to a torque shift of about 10 ppm during the measurement due to a change in B_0. This shows that the stability of the experiment was excellent and excludes significant random variations in the ambient field. During these measurements we logged the ambient AC field and found that the value did undergo one or two stepwise shifts of as much as 100 nT during a typical data collection period of 2.5 days for each datum. These shifts did not produce significant effects on the measurements. They could therefore have been due to magnetic disturbances at frequencies that were too high to be of consequence for the measurement or an instability in the gaussmeter.

5.2. Analysis of torque vs frequency

Figure 8 shows the measurements of the fractional change in torque due to the applied AC field as a function of frequency. In all cases the current flowing in the coil was 0.11A peak and

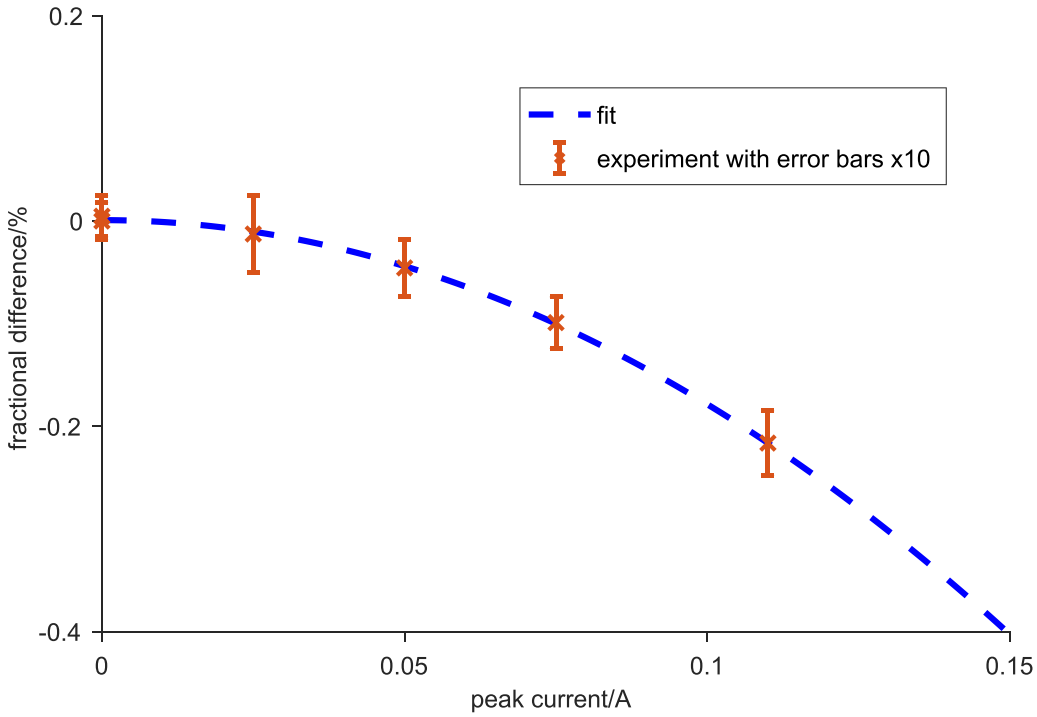

Figure 7. The fractional change in torque due to the amplitude of the alternating magnetic field as determined by the current passing through the coil. A peak current of 0.11 A corresponds to a rms field of 1 μT. The error bars representing 1 standard deviation are plotted with a magnification of a factor of 10.

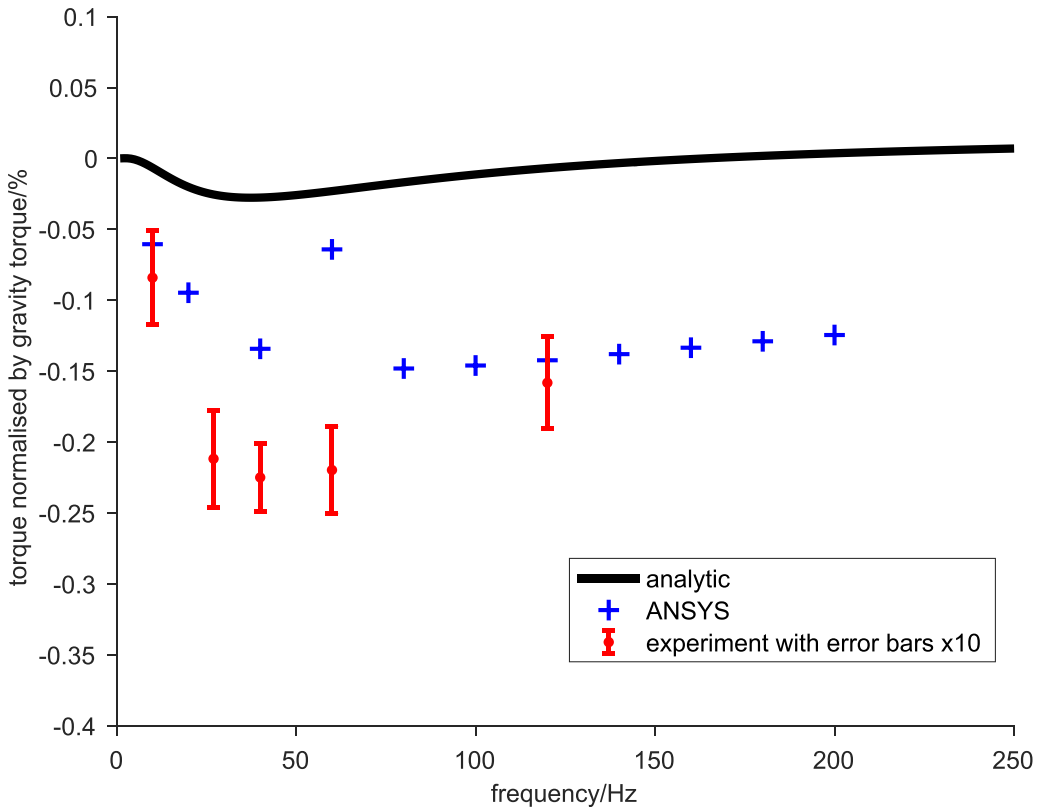

Figure 8. Plots of the measured torque vs frequency which are normalised to the Newtonian torque and expressed as a percentage. The 1 standard deviation uncertainties are magnified by a factor of 10. Also plotted are the results of the simple theory (including the vacuum can as a spherical shell) and the results of a FEA model with a cylindrical vacuum can in a uniform alternating magnetic field. The FEA model is labelled 'ANSYS' in the figure legend. As discussed in the text, the discrepancy between the experimental results and the analytical and FEA analyses is due to the inhomogeneity of the coil field.

this corresponded to a rms field at the magnetometer of about 1 μT. Also plotted is a theoretical curve that comes from the complete analytical model of the induced dipole interaction, including the effect of the vacuum can and assuming a uniform magnetic field with the value given at the centre of the coil. The calculated frequency dependency is modelled with the same test and source mass parameters used in figures 4 and 5. The vacuum can is modelled with the same parameters used for figures 6(a) and (b). Although the model gives a negative value of the torque and follows a similar shape as a function of frequency, the magnitude of the torque predicted by the analytical calculation is clearly much smaller. As discussed in section 3.3 the analytical model cannot accurately represent the attenuation of the field of the source masses due to the vacuum chamber (modelled as a spherical shell) and the model lacks the inhomogeneity of the coil field. As discussed in section 3.2, the inhomogeneity of the field would produce a repulsive force in the absence of the vacuum chamber and this would be expected to increase the 'dip' in the analytical curve

To further investigate the discrepancy between the theory and experiment a FEA model was used with a capped hollow cylindrical aluminium chamber, again, in an external uniform field equivalent in amplitude to that produced by the rectangular coil at its centre. The outer radius and external height were 153 and 420 mm respectively with a thickness of 4 mm. The conductivity was 1×10^7 S m^{-1}. The normalised torques are also shown as a function of frequency in figure 8. The point at 60 Hz is thought to be an anomaly due to the FEA program and was not investigated. The FEA results are closer to the experimental data. This can be understood as being due to the more precise calculation of the attenuation of fields due to the source masses by the vacuum chamber. Inclusion of the field inhomogeneity due to the coil would further increase the depth of the dip of the torque at the frequency of the measurement.

The analysis and measurements are therefore semi-quantitatively coherent and consistent with the physics of electromagnetism and a more detailed model was not pursued. Note that the vacuum chamber actually increases the torque in both analytical and FEA results and this can be understood as being due to the amplification of the external field being larger that the reduction in the internal fields as discussed in section 4. It should also be noted that this enhancement of the magnetic field exterior to the chamber only occurs with diamagnetic and not ferromagnet shields.

6. Possible torques from a compact oscillating magnetic dipole

In this section we will use the analytical and FEA models derived above to predict approximate magnitudes for torques that could arise from a localised oscillating dipole whose size is small compared with its distance from the torsion balance (a compact source). We can repeat the calculations for the uniform magnetic field, as described in the previous section, but now assume that the source magnetic field at a test or source masses is due to an arbitrary dipole $\vec{p}_g$ located at $\vec{r}_g$ is given by equation (18),

$$\vec{B}(\vec{r}) = \frac{\mu_0}{4\pi r_{s,t}^3}\left(3\vec{n}\left(\overrightarrow{n}\cdot\vec{p}_g\right) - \vec{p}_g\right), \tag{21}$$

where here $\vec{r}_{s,t} = \vec{r}_{s,t} - \vec{r}_g$, $r_{s,t} = |\vec{r}_{s,t}|$ and $\hat{n} = \frac{\vec{r}_{s,t}}{r_{s,t}}$. Figure 9 shows the torques that a compact dipole will produce on the torsion balance according to the FEA model and the analytical model. The results from analytical model are shown for the cases with and without the vacuum chamber. The dipole moment is scaled to give a rms magnetic field at the centre of the torsion balance of 0.7 μT and the dipole has a radial distance from the centre of the torsion balance of 1 m. The maximum amplitude of the torque with the vacuum chamber present corresponds to 0.15% change in the gravity torque. This torque is approximately equivalent to that of the coil discussed in section 5. We note that the torque can have both polarities but it is more probable for it to be positive.

7. Summary and discussion

The agreement between experiment and calculations described in the preceding sections suggests that the interaction between the masses in the BIPM determination of G and ambient alternating magnetic fields can be understood. The torques produced can give rise to biases in the value of G in an apparatus that is not magnetically shielded but the four-fold symmetry of the BIPM balance makes it largely insensitive to uniform fields. As can be seen from the experimental results made with the external coil and the calculation of the possible torques from a compact dipole, the sign of the torque is uncertain and rms fields of 1 μT give rise to torques of order 2000 ppm of either polarity. We have also observed that the magnitude of these torques scales as the square of the ambient magnetic field. The question then remains as to what values of field existed during the measurements made at BIPM in periods during the measurements leading to the publication of 2001 and 2013. The laboratory where the 2013 determination was performed has now been refurbished and the CMM used in this experiment has been relocated to the BIPM mechanical workshop. Measurements taken in 2018 on this CMM place an upper limit of 100 nT to the rms value of the ambient AC magnetic field. These measurements were made with the CMM actively moving its probe but, of course, no measurements of gravity torques during the experiments were made under these conditions. The direct measurements of ambient fields taken in Birmingham, as discussed in section 2, showed that the rms magnetic fields due to both compact sources and uniform fields were not greater than 10 nT.

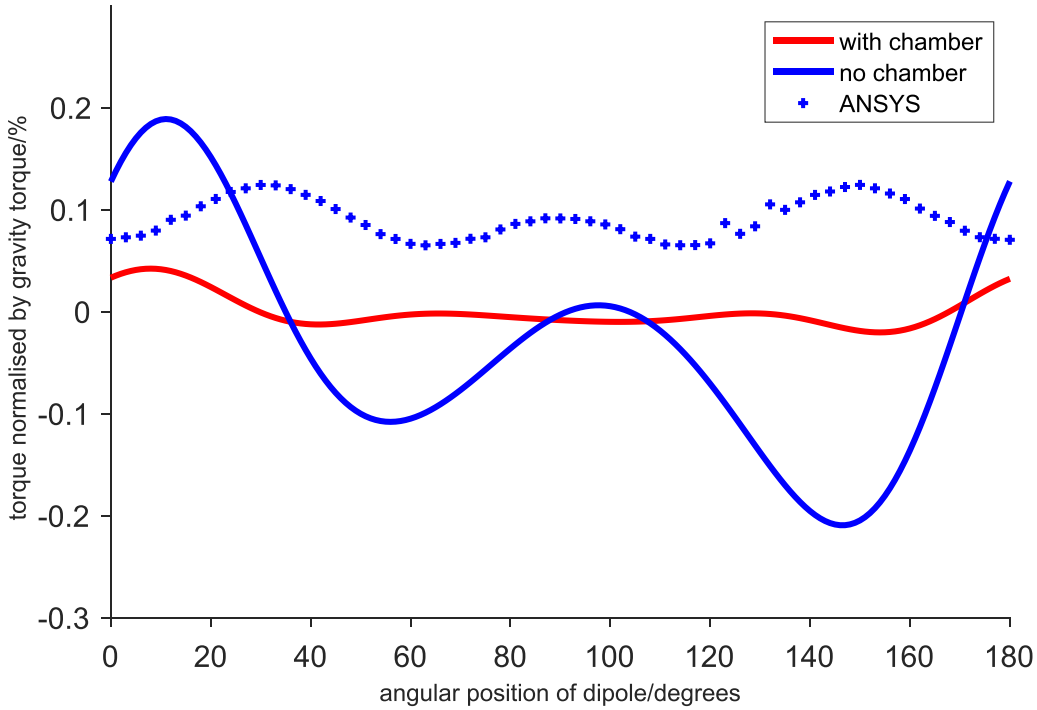

Figure 9. The calculated torque on the torsion balance due to a compact magnetic dipole as a function of its position on a circle of radius 1 m from the axis of rotation of the torsion balance. The magnitude of the dipole is chosen to give a rms magnetic field of 0.7 μT at the torsion balance. The FEA model is labelled 'ANSYS' in the figure legend. The other two curves are calculated using the analytical model described in section 5 but with a simple dipole field as a source. The analytical results are shown for the cases where the vacuum chamber is present or absent.

8. Conclusions

We have tested the hypothesis, put forward by the late Bryan Kibble, that the difference between the values of Newton's constant reported by BIPM in 2001 and 2013 and the currently accepted CODATA value was due to ambient alternating magnetic fields. Calculation shows that a uniform field creates no torque on an unshielded BIPM torsion balance if it has ideal four-fold symmetry. We have measured the torque on the BIPM apparatus produced by a coil, which is on a scale comparable with it, and observed a reduction in the gravitational torque, countering the intuition of Bryan Kibble. However analytical models and finite element analysis show that inhomogeneous fields can produce attractive or negative biases. Experimental results using the coil and modelling of the torques due a dipole at a distance of 1 m from the apparatus suggest that alternating magnetic fields of rms magnitude 1 μT at the balance can produce a bias in the torque of order ±0.2%. Experiments clearly showed that the torques scaled as the square of the amplitude of the ambient magnetic field, which is expected theoretically. Investigations of the ambient field in the environment of the CMM, used for the 2013 BIPM determination, suggest that typical rms fields at the location of the experiment were much less than 100 nT. Ambient fields in the laboratory in Birmingham had an rms magnitude of about 10 nT. These results therefore suggest such a bias would have been significantly below the level of 20 ppm for the BIPM G determinations. This is significantly smaller than the Type A uncertainties reported. A bias due to the spurious torques due to ambient magnetic fields cannot therefore resolve the discrepancy between the BIPM results and the CODATA recommended value. Any future attempts to significantly improve the accuracy of the determination using apparatus without magnetic shielding would need to take this source of bias into account.

Acknowledgments

We would like to thank Dr Sam Richman, Dr Harold Parks, Alain Picard (now passed) and all the BIPM staff who contributed to the two determinations of the Newtonian constant of gravitation, which spanned a period of some 20 years. We also thank Dr Pierre Gournay and Mr Philippe Roger for their valuable and essential assistance in making the measurements of the ambient AC magnetic fields of the CMM in the BIPM mechanical workshop. CCS would like to thank Dr Hasnain Panjani and Dr Ludovico Carbone, who initially set up the BIPM torsion balance in Birmingham, and Peter Steele and Mark Gilbert who, as fourth year undergraduate students, started the work reported here. CCS would also like to thank Dr Chris Collins, Dr Stephan Schlamminger (NIST), Dr David Newell (NIST) and Dr Julian Stirling for useful discussions.

ORCID iDs

Clive C Speake https://orcid.org/0000-0002-2031-7449
John L Bryant https://orcid.org/0000-0002-7243-3230
Richard S Davis https://orcid.org/0000-0002-0246-8163
Terry J Quinn https://orcid.org/0000-0001-8308-1261

References

[1] Quinn T J, Speake C C, Richman S J, Davis R S and Picard A 2001 A new determination of G using two methods *Phys. Rev. Lett.* **87** 111101

[2] Quinn T, Speake C, Parks H and Davis R 2014 The BIPM measurements of the Newtonian constant of gravitation, G *Phil. Trans. R. Soc.* A **372** 2–28

[3] Tiesinga E, Mohr P J, Newell D B and Taylor B N 2021 Codata recommended values of the fundamental physical constants: 2018 *J. Phys. Chem. Ref. Data* **50** 033105

[4] Rothleitner C and Schlamminger S 2017 Invited review article: measurements of the Newtonian constant of gravitation, G *Rev. Sci. Instrum.* **88** 111101

[5] Speake C and Quinn T 2014 The search for Newton's constant *Phys. Today* **67** 27–33

[6] Mohr P J, Newell D B and Taylor B N 2016 CODATA recommended values of the fundamental physical constants: 2014 *J. Phys. Chem. Chem. Ref. Data* **45** 043102

[7] Wu J, Li Q, Liu J, Xue C, Yang C, Shao S and Luo J 2019 Progress in precise measurements of the gravitational constant *Ann. Phys., Lpz.* **531** 2–28

[8] Quinn T, Parks H, Speake C and Davis R 2013 Improved determination of G using two methods *Phys. Rev. Lett.* **111** 101102

[9] Private communication via James E. Faller

[10] Griffiths J G 1999 *Introduction to Electrodynamics* 3rd edn (Upper Saddle River, NJ: Prentice Hall) p 282

[11] Smythe W R 1989 *Static and Dynamic Electricity* 3rd edn (London: Taylor and Francis) pp 374–7

[12] Jackson J D 1999 *Classical Electromagnetism* 3rd edn (New York: John Wiley and Sons) p 219

[13] Jackson J D 1999 *Classical Electromagnetism* 3rd edn (New York: John Wiley and Sons) p 186